Mechanical, Flammability, and Crystallization Behavior of Polypropylene Composites Reinforced by Aramid Fibers

Xiaosui Chen,[1,2,3] Sheng Zhang,[1,2,3] Guozhi Xu,[4] Xinjun Zhu,[5] Wei Liu[6]

[1]*Key Laboratory of Carbon Fiber and Functional Polymers, Ministry of Education, Beijing University of Chemical Technology, Beijing 100029, China*
[2]*Preparation and Processing of Novel Polymeric Materials, Beijing University of Chemical Technology, Beijing 100029, China*
[3]*State Key Laboratory of Chemical Resource Engineering, Beijing University of Chemical Technology, Beijing 100029, China*
[4]*Department of Materials Science and Engineering, Beijing Technology and Business University, Beijing 100037, China*
[5]*Heilongjiang Hongyu New Material of Short Fiber Limited Company, Heilongjiang Province 154004, China*
[6]*Sichuan Fire Research Institute of Ministry of Public Security, Dujiangyan 611830, China*

Received 11 January 2011; accepted 10 May 2011
DOI 10.1002/app.34868
Published online 6 January 2012 in Wiley Online Library (wileyonlinelibrary.com).

ABSTRACT: In this article, we report the mechanical and thermal properties, together with the crystallization and flammability behaviors, of pure polypropylene (PP) and PP/aramid fiber (AF) composites with AF loadings of 5, 10, 20, 30, and 40 wt %. The mechanical properties of the samples were evaluated by tensile and izod notched impact tests, and the results show that the tensile strength of the composites could reach up to 67.8 MPa and the izod notched impact strength could rise to 40.1 kJ/m^2. The structure and morphology were observed by scanning electron microscopy and polarized optical microscopy, respectively. This demonstrated that a solid interface adhesion between the matrix and fibers was formed. The thermal and crystalline behaviors of the PP/AF composites were also investigated by thermogravimetric analysis and differential scanning calorimetry analysis, and the results show that the char residue of the PP/AF composites improved greatly with increasing AF loading, and the highest value could reach up to 23.7% in the presence of 40 wt % AF. The supercooling degree, initial crystallization temperature, and crystallization percentage were used to characterize the crystallization behavior of the PP/AF composites, and the results indicate that the AFs had positive effects on the promotion of PP nucleation, which can usually improve the mechanical properties of composites. Moreover, the flammability analysis of the PP/AF composites demonstrated that the presence of AFs could significantly decrease the peak heat release rate and the total heat release and reduce the melt-dripping of the PP/AF composites. © 2012 Wiley Periodicals, Inc. J Appl Polym Sci 125: 1166–1175, 2012

Key words: crystallization; fibers; flame retardance; poly(propylene) (PP); reinforcement

INTRODUCTION

Polypropylene (PP) has a prominent position among all commodity polymers because of its excellent price/performance ratio, numerous possibilities for modifying its structure, and good recycling; it has been widely used in the fields of household appliances, vehicles, packaging, architecture, and so on. However, several disadvantages of PP, such as a mechanical strength deficiency, molding shrinkage, and a low thermal deformation temperature, make it inadequate for many applications. Therefore, considerable efforts have been undertaken to try to improve these deficiencies.[1–5]

Attempts at adding commanded inorganic rigid particles, elastomers, and fibers have been adopted to reinforce the polymer resins.[6–8] Recently, fiber-reinforced polymer composites have attracted a lot of attention because of their ease of fabrication, economy, and superior mechanical properties. Extrusion and injection-molding processes are common ways employed to prepare the related composites.[3] Various fibers, such as glass fibers,[9] aramid fibers (AFs),[10] carbon fibers,[11] wood, hemp, and their hybrids, have already been considered as reinforcing materials to satisfy the required commercial performance requirements. However, short AFs have rarely been used to make composite materials with the PP matrix, where glass fibers are usually preferred. Many efforts have been made to investigate the effects of glass fibers on the mechanical properties,[12–15] crystallization behavior,[16–18] and interfacial structure[19–21] of PP composites.

Correspondence to: S. Zhang, College of Materials and Engineering, Mailbox No. 2, Beijing University of Chemical and Technology, Beijing 100029, China (sheng1999@yahoo.com) or G. Zu (xgzhi@th.btbu.edu.cn).

Contract grant sponsor: National Natural Science of China; contract grant numbers: 20974009/B0402, 21061130552/B040607.

The efficiency of fiber reinforcement is dependent on many variables, for example, the quantity and dispersion,[22] length,[23–25] shape,[26] and orientation[27] of fibers in the resin matrix, whereas the most important one is the interfacial adhesion between the reinforcing fibers and the polymer matrix.[28,29] To achieve optimal reinforcement, the surface modification of fibers with chemicals or physical treatments is applied. Under appropriate conditions, a highly oriented crystalline layer, called *transcrystallization*, can form at the fiber/matrix interface in composites when a semicrystalline polymer is used as the matrix; this develops from the perturbation of the crystallization rate, which is induced at the fiber surface and propagated away form the fiber surface in the matrix.[30] The structure and size of transcrystallization differs from the fiber type and size, coupling agents, and surface morphology of the fibers.[31,32] Cui[33] reported that the interfacial adhesion among the fibers and matrix has a great influence on the generation of transcrystallization. If the interfacial adhesion is too weak to make polymer chains orientate along fibers, the transcrystallization cannot be formed. However, if the adhesion is too strong and the cooling rate is very fast, there is no obvious difference in the crystallization rate between the polymer chains around and away from fibers, and therefore, the PP spherulites can grow across fibers with no transcrystallization at all. However, the effect of transcrystallization on the mechanical properties of polymer/fiber composites is still controversial.[32,34]

It has been reported that the crystallization kinetics of crystalline thermoplastic polymer matrices can be greatly altered in the presence of fibers. Under certain conditions, fibers inserted into a polymer matrix can act as heterogeneous nucleating agents and, thus, improve the degree of crystallization and decrease the spherulite size and the half-crystallite time of the polymer matrix compared with the one in the bulk.[35]

As is well known, AFs have excellent properties and a high thermal stability; they are good candidates as reinforcing materials and are widely used in rubbers and plastics. Many authors[3,35–38] have reported the reinforcement of mechanical and crystalline properties in detail, but the effects on the thermal and flaming properties are nearly nonexistent. In this study, we investigated the mechanical, crystalline and thermal properties together with the flammability of PP composites reinforced by AFs using characteristic techniques, including tensile and izod notched impact tests, scanning electron microscopy (SEM), polarized optical microscopy (POM), thermogravimetric analysis (TGA), differential scanning calorimetry (DSC), limiting oxygen index (LOI) testing, and UL-94 testing.

TABLE I
Compositions of the PP/AF Composites (w/w)

Sample	Fiber loading (%)	Antioxidant loading (%)
PP	—	0.5
PPAF1	5	0.5
PPAF2	10	0.5
PPAF3	20	0.5
PPAF4	30	0.5
PPAF5	40	0.5

EXPERIMENTAL

Materials

PP (K1001) was supplied by Yan Shan Petroleum Co., Ltd. (Beijing, China). Antioxidant B225 was obtained from Beijing Dilong Chemical Industry Co., Ltd. (Beijing, China). The chopped-surface-modified AFs (Aramid fibers, Kevlar 1414), with a diameter of 12 μm and a length of 3 mm, were provided by Heilongjiang Hongyu New Material of Short Fiber Co., Ltd. (China). All of the experimental materials, including PP, AF, and process additives, were dried overnight in an oen at 80°C before they were processed.

Sample preparation

The PP/AF composites were melt-prepared by the blending of PP with different loadings of chopped fibers and antioxidants in a two-screw extruder (F-1, Shanghai, China) in the temperature range 160–200°C with a screwing speed of 100 rpm. The antioxidants (0.5% w/w) were added to prevent the polymer from degrading at high temperature. The extruded materials were cooled directly at the exit of the extruder in water and were then subsequently pelletized. The pelletized samples were molded into specimen size at 180–190–180°C for further analysis and tests with a plastic injection-molding machine (A-80-210-4, Auckland industrial Co., Ltd. Hongkong, China). The formulations of the PP/AF composites are given in Table I.

Mechanical properties

The tensile properties of the composites (dumbbell-shaped, span length = 50 mm, width =10 mm, thickness = 4 mm) were characterized by a computerized universal testing machine (L R30 K PLUS, Lloyd, United Kingdom) at a speed of 50 mm/min according to GB/T1040-1992. The izod notched impact tests (sample dimensions: $80 \times 10 \times 4$ mm^3) were done with a Resil Impactor (P/N 6957, CEAST, Italy) under an impact power of 25 J according to GB/T1843-1996. All samples were tested five times, and the average values were used as the final data, with a variance of ±5%.

DSC analysis

The crystallization properties of the composites were examined with a Shimadzu DSC-60 instrument (Japan) with samples of 3–5 mg in the temperature range 50–200°C under a flow in nitrogen (30 mL/min) atmosphere. The samples were first heat to 200°C at a heating rate of 20°C/min, maintained at this temperature for about 5 min to eliminate the previous thermal history, then rapidly cooled down to room temperature at a cooling rate of 20°C/min, and finally heated up to 200°C at that rate again. The data of exothermic and endothermic enthalpy and the peak temperature were calibrated with indium and zinc according to ASTM D 3417 and ASTM D 3418 in the testing process.

Wide-angle X-ray diffraction (WAXD) analysis

The WAXD analysis was conducted with a D/max-2500 diffractometer (Rigaku Corporation, Japan) (Cu Kα radiation, $\lambda = 0.154$ nm, reflection mode) at room temperature. The samples were obtained form the molding materials with dimensions of $10 \times 10 \times 3$ mm^3. The diffraction angle (2θ) scanning range was 5–40°C, with a rate of 1°/min. The content of β-phase modification (K_β) was calculated according to the well-known Turner–Jones formula:[39]

$$K_\beta = H_\beta(300)/[H_\alpha(110) + H_\alpha(040) + H_\beta(300) + H_\alpha(130)]$$

where $H_\Omega(hkl)$ is the intensity of the (hkl) peak belonging to phase Ω, respectively.

SEM analysis

The fractured samples gained from izod notched impact testing were first carbon-coated and then observed in an SEM instrument (S-4700, Hitachi, Japan).

POM analysis

The crystalloid microstructures of the pure PP and reinforced PP composites were characterized by POM (SM-LUX-POL, Leitz, Germany). All of the samples were first cut into slices, then heated up to 200°C, held for 10 min, and then cooled down to room temperature at 20°C/min. The microphotos of the PP spherulites were taken with a magnification of 200×.

The fiber lengths of the AFs before and after extrusion were also investigated by POM. First, the selected samples were put into a muffle furnace at 350°C for 1 h to remove the PP matrix by thermal degradation and were then dropped into a glass beaker filled with concentrated sulfuric acid to react and dissolve the residual char. Third, the solution was filtered *in vacuo* after it had been diluted with distilled water. Finally, the fibers were successfully obtained and observed under a POM analyzer with a magnification of 40×.

TGA

TGA was performed in a TGA instrument (HCT-1, Beijing Hengjiu Instrument, Ltd., China) with a heating rate of 10°C/min in a temperature range of 50–800°C under static air conditions. The mass of each sample was approximately 3–5 mg.

Flammability properties

The LOI test was carried out on a JF-3 type instrument (Jiangning Nanjing Analytical Instrument Factory, China) with dimensions of $120 \times 6.5 \times 3$ mm^3 according to GB/T 2406-1993. The UL-94 test was done with an apparatus for burning tests (vertical and horizontal) with a CZF-3 instrument (Jiangning Nanjing Analytical Instrument Factory, China) with dimensions of $125 \times 12 \times 3$ mm^3, according to GB/T 2408-1996.

The combustion behavior of the PP/AF composites was evaluated by a cone calorimeter (FTT0007, Fire Testing Technology Co., United Kingdom) according to ISO 5660. Square specimens were irradiated at a heat flux of 50 kW/m^2 with dimensions of $50 \times 50 \times 3$ mm^3.

RESULTS AND DISCUSSION

Mechanical behaviors

Figure 1 shows the tensile strengths of PP/AF composites with different AF loadings. It was seen that

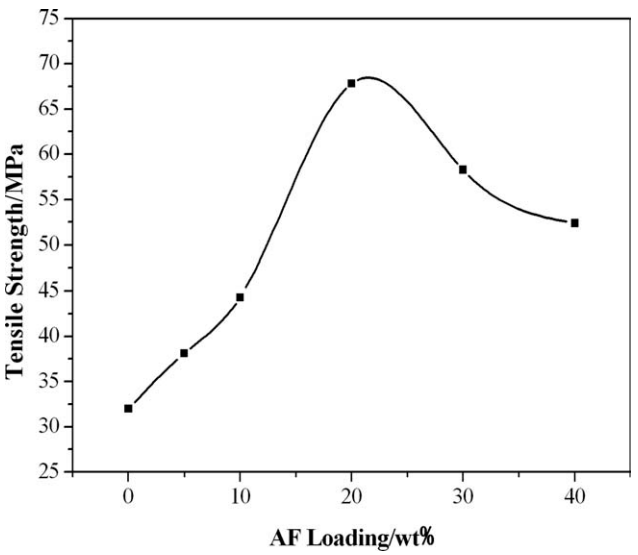

Figure 1 Tensile strength of the PP/AF composites.

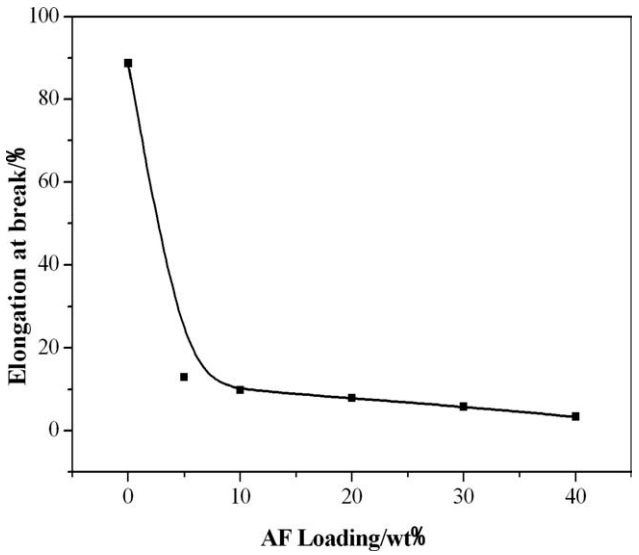

Figure 2 Elongation at break of the PP/AF composites.

the tensile strength of the composites increased greatly at first and then decreased slightly, reaching a highest value of 67.8 MPa, which was 111.8% higher than that of pure PP. As to the elongation at break of the composites shown in Figure 2, it dropped straightly relative to the increase in AF loading. It is well known that there is a fiber-bridging effect in fiber-reinforced polymer composites that can undertake the major portion of the external energy. Moreover, the energy can be transferred well through the interfacial adhesion between PP and fibers and can then be scattered homogeneously in a bigger volume, by which the power-bearing capability of the whole composite is improved significantly. Therefore, the interfacial adhesion between the fibers and PP matrix played a significant role in improving the mechanical properties of PP/AF composites. However, the tensile strength decreased when the fiber loading exceeded the critical value of 20 wt %. The overloading AF could reduce the processability of the PP/AF composites, and thus, AF could not be dispersed homogeneously and impregnated completely in the PP matrix. The agglomeration of AF caused stress concentration and decreased the capability of the energy spreading severely, which finally led to a lower tensile strength.[10,23,40] Moreover, the mechanical properties of the polymer/fibers composites were also affected by the fiber length.[41] Figure 3 shows the POM pictures of AFs before and after extrusion. It could be seen that the AF fibers taken from samples PPAF1 and PPAF5, shown in Figures 3(b) and 3(c), respectively, were much thicker than the original AF fiber, shown in Figure 3(a); this could have been due to the swelling of AFs after the absorption of water during sample preparation. The fiber length of sample PPAF5 was shorter than that of sample PPAF1, but both of them were much shorter than the original AFs; this indicated that the fiber length decreased with increasing fiber content. However, the shortening of fiber length was mainly caused by fiber breakage during extrusion, which could

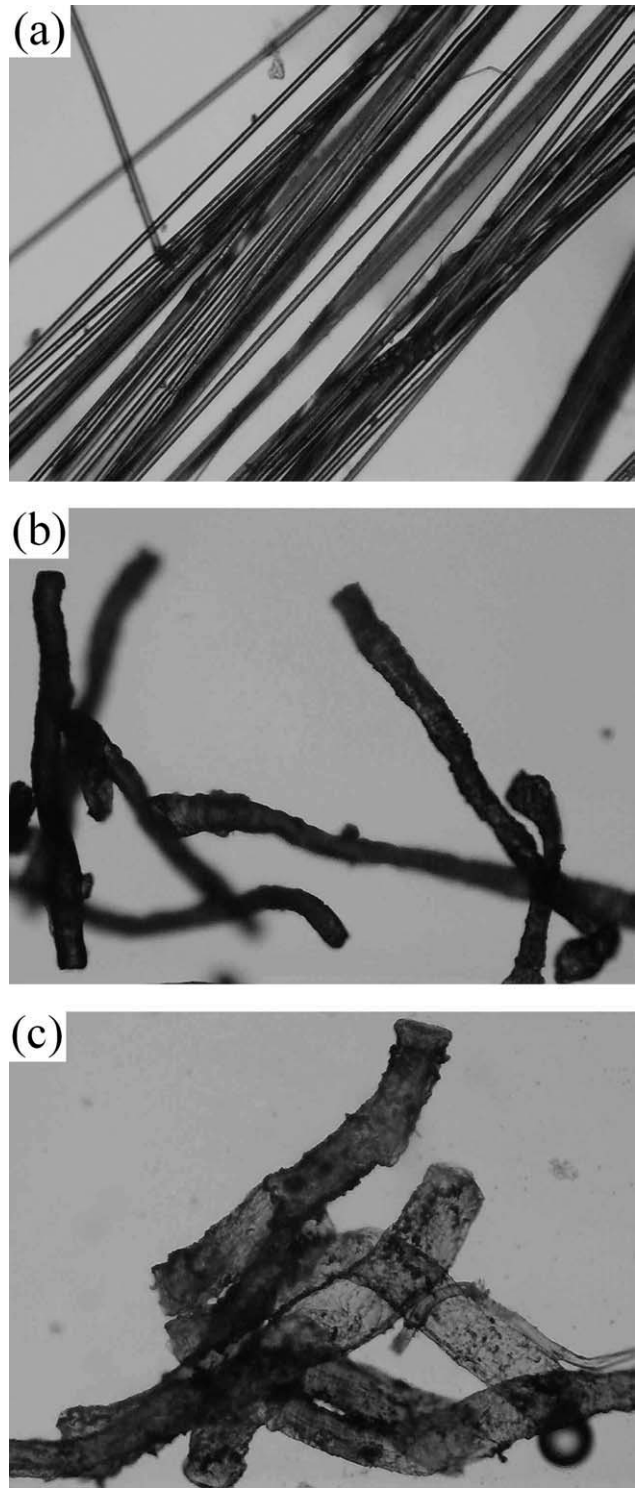

Figure 3 POM pictures of AF before and after extrusion with a magnification of 400×: (a) AF before extrusion, (b) AF from PPAF1, and (c) AF from PPAF5

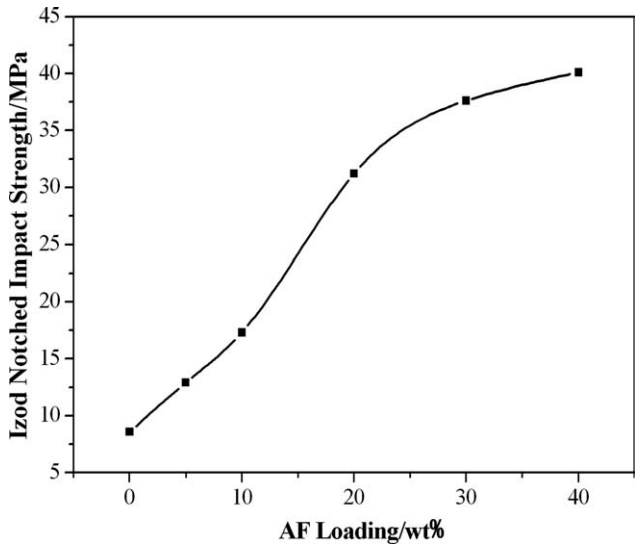

Figure 4 Izod notched impact strength of the PP/AF composites.

decrease the strengthening efficiency of AFs in the PP composites.[42]

Figure 4 shows the izod notched impact strengths of the PP/AF composites with different AF loadings. It was found that the impact strength kept increasing and reached a highest value of 40.1 kJ/m^2 with 40 wt % AF; this was approximately 3.7 times bigger than that of pure PP and indicated that the impact properties of the PP/AF composites were obviously strengthened in the presence of AFs. It has been suggested that the impact power is absorbed in fiber-reinforced composites by three main types: fiber breakage, fiber pullout, and matrix distortion, which is shown in Figure 5. The second type mainly appears in composites with poor compatibility between the fibers and polymer matrix, whereas the first type usually occurs when good interfacial adhesion forms between the fibers and matrix; this is very desirable in fiber-reinforced composites. When the external power was addressed on the samples, it could be transferred and passed along the interweaving fibers (i.e., scattering power), which could improve the capability of external power bearing. Moreover, fibers can form a net structure in the composites, which can increase the effective length of AFs.[3] It has been reported that the mechanical properties of PP/AF composites are higher when the effective length is longer.

Figure 6 shows the SEM micrographs of the fractured surfaces of PP/AF composites containing different AF loadings. It can be seen that whereas there were many drawing wires attached to fibers and few holes of fiber pullout observed in the fractured surfaces of the PP/AF composites, the pure matrix's fracture surface was very brittle; this indicated that good interfacial adhesion and bonding between the fibers and PP matrix were formed, which played an important role in improving the mechanical properties of the PP/AF composites.[3] It was also clearly seen that the AFs were already dispersed homogeneously in the PP/AF composites; this was also an important factor in enhancing the mechanical properties of the reinforced composites.

Figure 7 shows the POM pictures of the PP/AF composites. It is well known that PP has a nice capability of crystallization. As shown in Figure 7(a), the pure PP's spherulites were quite big and integrated with many Maltese crosses, as clearly shown. However, when we compared these six POM pictures, it was obvious that the spherulites of PP became smaller gradually and were also arrayed densely along with increasing AF loading in the PP/AF composites; this had a good effect on improving the mechanical properties. It was possible because the AFs could act as heterogeneous nucleation agents and, hence, could form more nucleating points in the reinforced PP composites. Thus, when plenty of crystal nucleuses grew simultaneously, the PP spherulites developed into smaller and more integrate ones, and then, fewer defect spherulites occurred, and better mechanical properties were obtained.

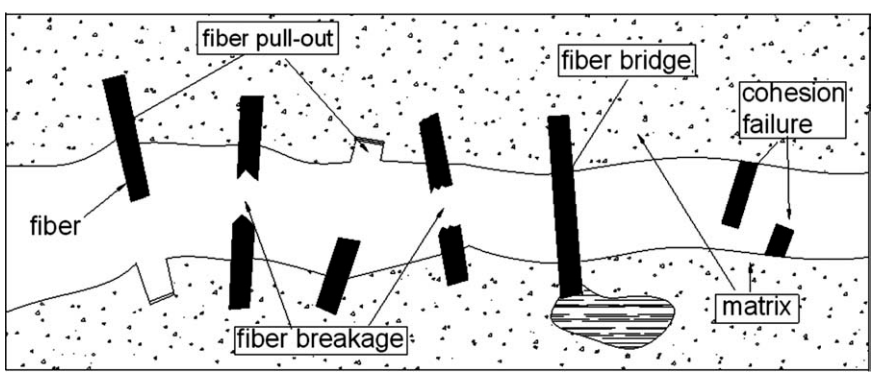

Figure 5 Three main types of absorbing impact power of the fiber-reinforced composites.

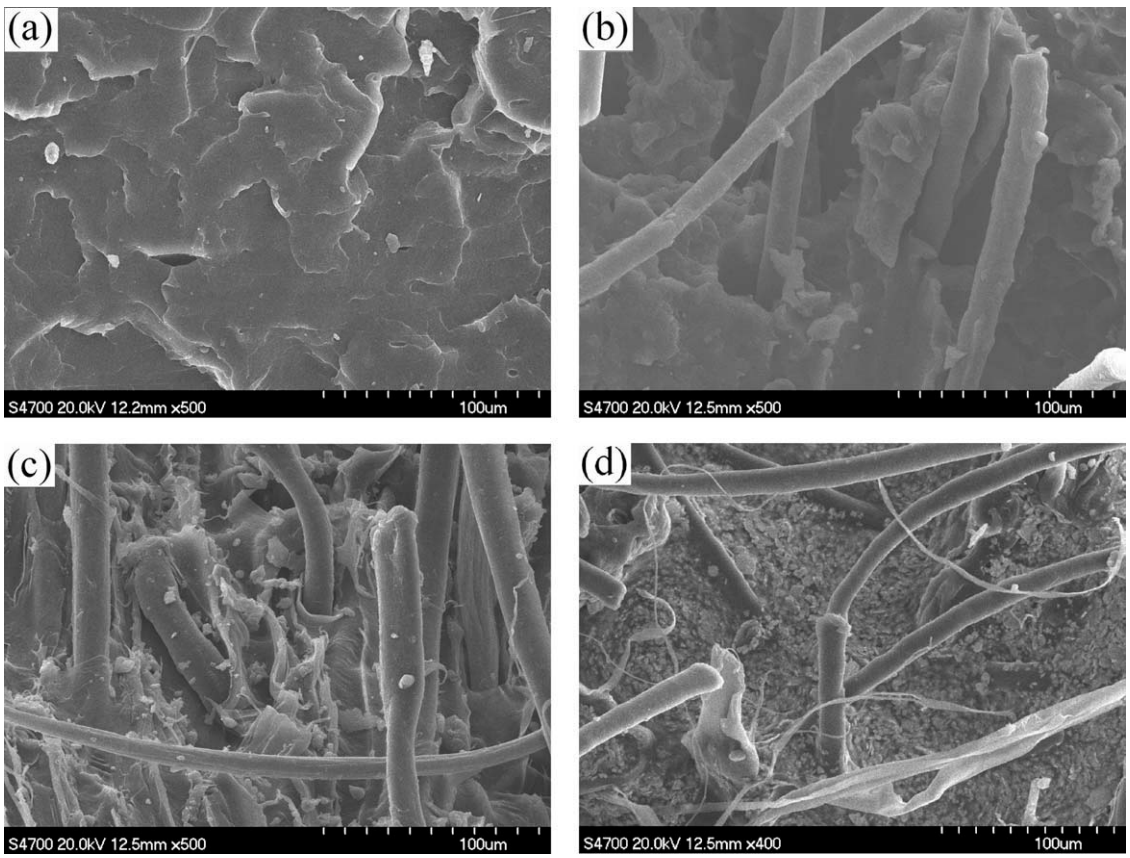

Figure 6 SEM micrographs of the fractured surface of the PP/AF composites and pure PP: (a) PP, (b) PPAF1, (c) PPAF2, and (d) PPAF3.

WAXD analysis

It is well known that PP can form four crystal phases: α-monoclinic, β-hexagonal, γ-triclinic, and δ in different environmental conditions. The monoclinic α phase with a cross-hatched lamellar structure is predominantly formed, and it shows the best stability among these crystal systems.[43] However, the β phase of PP has a higher distortion temperature and better impact properties compared with the α phase, and thus, a higher K_β is desired. K_β can be increased with additional β-nucleation agents or under certain shearing conditions. The microstructure of the PP crystals was investigated with WAXD analysis. Figure 8 shows the X-ray diffractograms of the pure PP and PP/AF composites. The 2θ values of different crystal phases and K_β are list in Table II. The diffraction peaks at 2θ's of 13.8° (α_{110}), 16.6° (α_{040}), and 18.4°(α_{130}) were the principle reflection of the α phase of the PP crystals, whereas the diffraction peak at a 2θ of 15.8° (β_{300}) was the characteristic reflection of the β phase of the PP crystal.[44,45] It was obvious that there was no change in crystal forms whether the AF was added or not in the PP composites. However, the intensity of the β phase (β_{300}) was enhanced, whereas that of the α phase weakened, with increasing AF loading in the PP/AF composites. Moreover, the value of K_β also showed the same tendency, reaching a maximum value of 20.0% with an AF loading of 40 wt %; this value was much higher than that of pure PP. This indicated that the AF could act as a β-nucleating agent for PP crystallization in the PP/AF composites.

Crystallization and melt behavior analysis (DSC)

The crystallization and melting behavior of the PP/AF composites were analyzed by DSC, as shown in Figures 9 and 10, respectively. It is obvious that the trace of β-fusion peaks could not be observed in the melting curves of DSC. This may have been related to the different preparation processes of these two experimental samples. It has been reported that because of the lower stability of the β phase in comparison with the α phase, the β phase occurs sporadically and can only be formed under some critical conditions, such as the quenching of the melt to a certain temperature range, directional crystallization in a thermal gradient field, shearing or elongation of the melt during crystallization, vibration-induced crystallization, or the use of β-nucleating agents.[45] The samples used for the WAXD tests were directly obtained from molding samples, which were

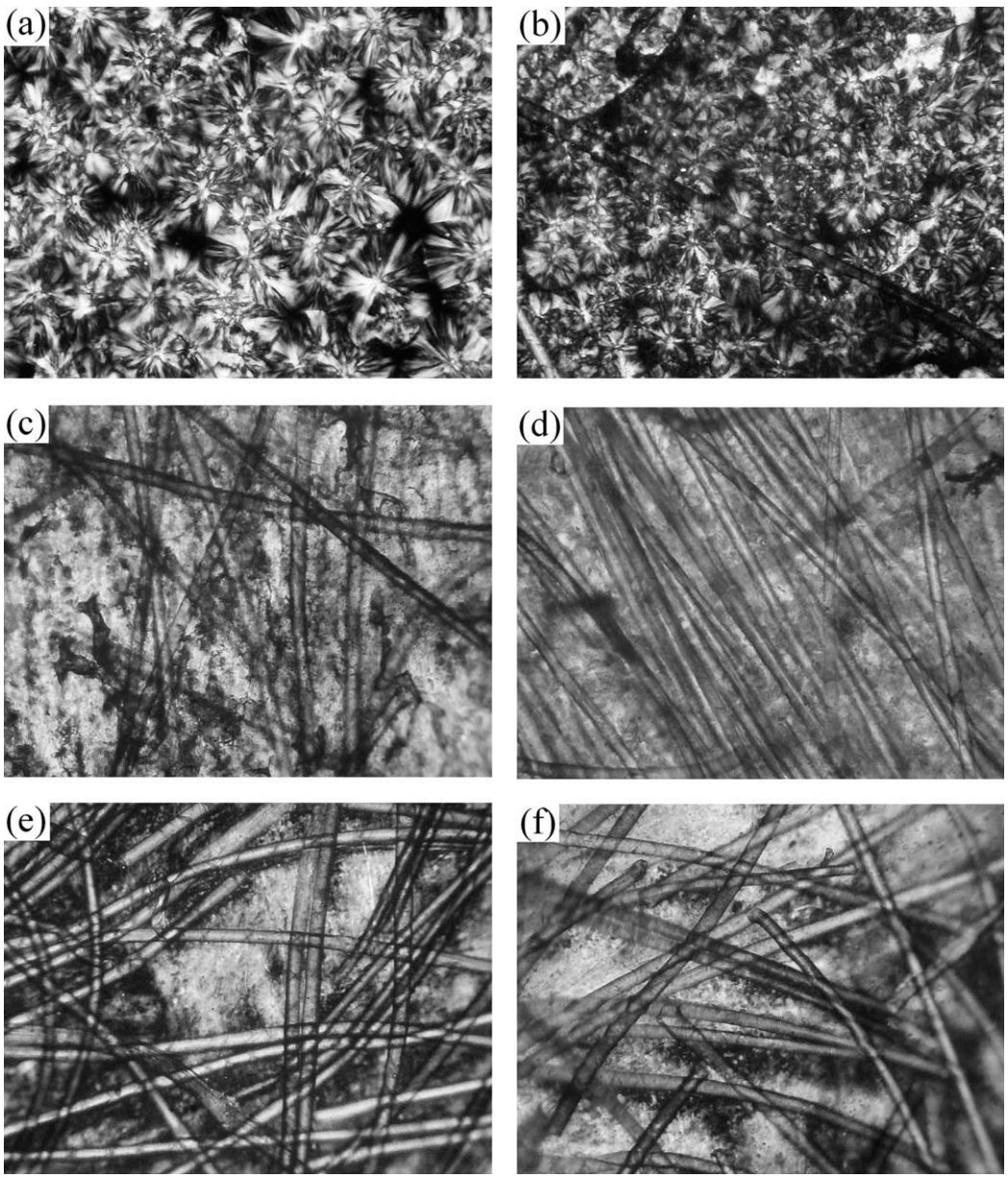

Figure 7 POM pictures of pure PP and some of the PP composites: (a) PP, (b) PPAF1, (c) PPAF2, (d) PPAF3, (e) PPAF4, and (f) PPAF5.

prepared by the quenching process, whereas the samples used for the DSC tests were recrystallized and melted in a relatively slow thermal gradient. The presence of AFs had a positive effect on increasing K_β which had a maximal value of 20%. Therefore, it was difficult to form the β phase in the DSC test or at low contents; this was also supported by Maity et al.[3]

The detailed parameters obtained from these curves, including initial crystallization temperature (T_{ic}), crystallization peak temperature (T_c), melting peak temperature (T_m in the second heating course), supercooling degree ($\Delta T = T_m - T_c$), and crystallization peak width at half-width ($W_{H/2}$) are summarized in Table III. Under nonisothermal conditions, T_{ic} and ΔT reflect the ability of nucleation and the rate of crystallization.[46] It was seen that the value of T_{ic} increased, but the value of ΔT decreased, in the PP/AF composites with increasing AF addition; this indicated that the AFs had a positive effect on promoting the nucleation of PP and increasing the rate of crystallization at the same time.[47] Moreover, $W_{H/2}$,[48] which is also related to the rate of crystallization, revealed the same developing tendency as that of ΔT. This also could have been due to the nucleating ability of the AFs for improving the crystallization behavior of PP. With the increasing loading of AFs in the PP/AF composites, more and more

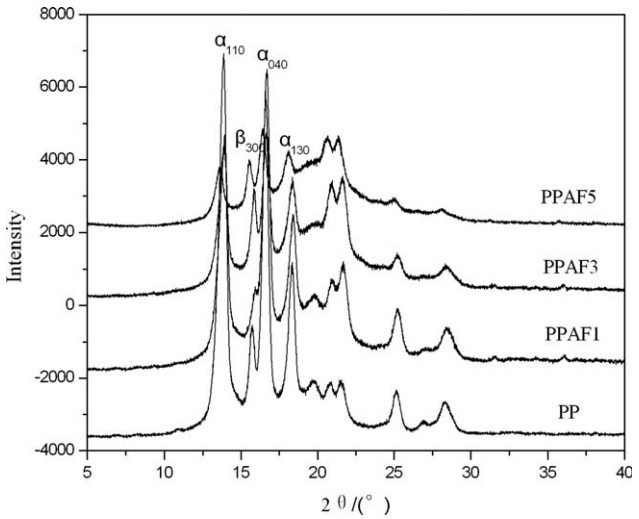

Figure 8 WAXD diagrams of the pure PP and PP/AF composites.

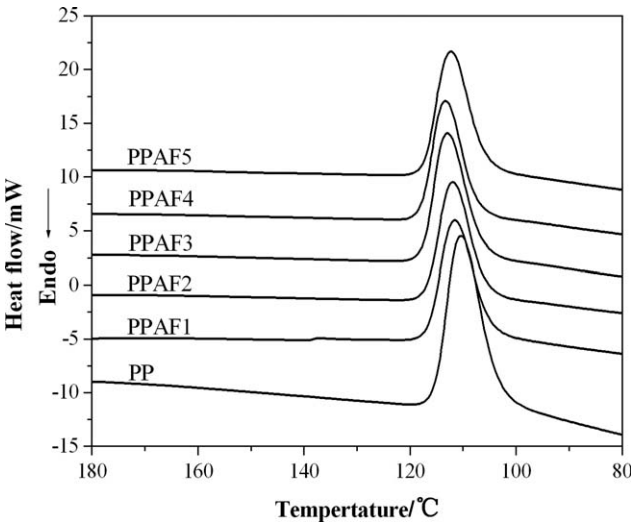

Figure 9 DSC cooling curves of the pure PP and PP/AF composites.

PP molecular chains oriented along the added fibers, which made it easy for PP to crystallize. PP spherulites could first grow along the AFs and then spread to the others away from the fiber center.[38] Besides, the good ability of AFs in nucleating could have also made the crystallization much easier. These can be explained by the reduced value of the melting enthalpy (ΔH_m) of the crystallizaion peak shown in Table III.

The percentage of crystallization (X_c) calculated from DSC was determined by the following equation:

$$X_c(\%) = \Delta H_m \times 100/(\Delta H_m^0 \times m)$$

where the value of ΔH_m^0 is 209 J/g which is standard heat of melting of 100% crystalline PP[3] and m is the mass fraction of PP in the PP/AF composites. As shown in Table III, X_c increased slightly at first and then rapidly with increasing fiber loading. This suggested that the fiber surface could act as nucleation sites for PP crystallization, so when a small amount of fibers were added to the composites, the fibers may have prevented the movement of PP chains and, thus, decreased the number of nucleation sites. However, when the fiber loading exceeded a certain level, plenty of nucleation sites occurred and played an active role in the crystallization of PP over the blocking effect.[48]

TABLE II
2θ and K_β Values of the PP and PP/AF composites

Sample	2θ of α_{110} (°)	2θ of β_{300} (°)	2θ of α_{040} (°)	2θ of α_{130} (°)	K_β (%)
PP	13.8	15.7	16.6	18.4	6.5
PPAF1	13.9	15.9	16.6	18.4	8.3
PPAF3	13.9	15.8	16.6	18.4	14.8
PPAF5	13.6	15.6	16.5	18.2	20.0

TGA

The TGA curves of the pure PP, AFs, and PP/AF composites are shown in Figure 11, and detailed data obtained from these curves are list in Table IV. It is shown that pure PP decomposed in one step in the temperature range 271.3–400.4°C, whereas the AFs decomposed in the temperature range 503.2–707.6°C. All of the PP/AF composites had two steps of decomposition, with the first one corresponding to pure PP's degradation and the second one corresponding to AF degradation. The onset degradation temperatures of all of the PP/AF composites were already decreased in different degrees (ca. 10°C); this could have been due to the degradation of surface modifier covering the fibers' surface. The char residue in Table IV showed a gradual enhancement, which was relevant to the increasing mass level of

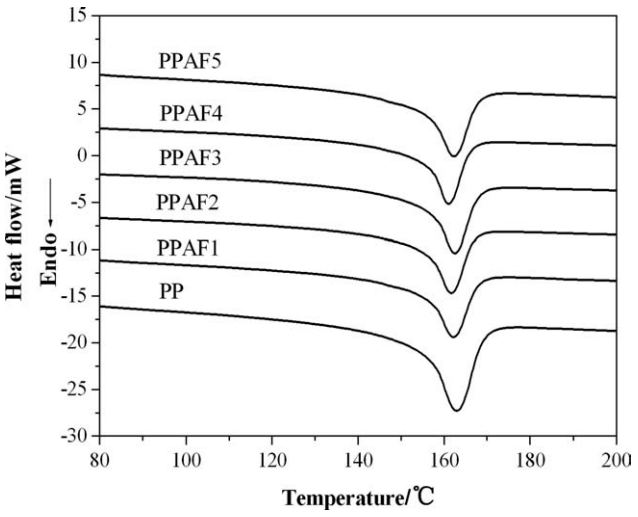

Figure 10 DSC melting curves of the pure PP and PP/AF composites.

TABLE III
Crystallization and Melt Parameters of the PP/AF Composites

Sample	T_{ic} (°C)	T_c (°C)	T_m (°C)	ΔT (°C)	ΔH_m (J/g)	X_c (%)	$W_{H/2}$ (°C)
PP	118.6	110.1	163.3	53.2	−73.18	35.01	7.37
PPAF1	120.5	111.4	162.3	50.9	−70.50	35.42	7.22
PPAF2	121.0	112.2	161.7	49.5	−67.95	35.77	6.80
PPAF3	121.42	113.1	162.3	49.2	−63.81	36.64	6.77
PPAF4	121.87	113.4	161.0	47.6	−62.58	38.92	6.75
PPAF5	121.42	112.5	161.8	49.3	−57.57	38.56	6.78

AFs in the PP/AF composites; this indicated that the AFs had a positive effect in enhancing the char yield of the PP/AF composites. The AFs had excellent thermal stability, and they started to decompose only after 500°C. When the heating temperature was lower than the critical decomposition temperature of the AFs, the fibers could act as a protective cover, surrounding the PP chains and, thus, delaying the heat spreading. However, when the heating temperature was higher than that one, the AFs could form char layers easily because of their special structure and cover the PP surface; this could still hinder the exchange and spreading effect of heat and oxygen. Therefore, the PP/AF composites had better thermal stability and higher char residue than the pure PP.

Flammability properties

The experimental results of LOI and UL-94 vertical burning tests are shown in Table V. It is clear that none of the samples achieved a UL-94 rating because of the relatively long burning times, despite the fact that the LOI value of the PP/AF composites was slightly increased in comparison with that of the pure PP. However, melt-dripping was not be observed for the PP/AF samples during the vertical burning test. This suggested that the thermally stable AF acted as a skeleton in the PP/AF composites and prohibited the melting flow of the PP matrix during combustion and formed compact char layers which could cover over the PP surface and thus hinder the spreading effect of heat and oxygen. Therefore, AF played positive effects on promoting the flame retardancy of the PP/AF composites.

Figure 12 shows the heat release rate (HRR) curves of PP, PPAF3, and PPAF4, respectively. The time to ignition of the three samples was very similar, but the time to peak heat release rate (PHRR) varied greatly. It took 80 and 90 s for samples PPAF3 and PPAF4 to get to PHRR, respectively, whereas pure PP needed only 65 s. Moreover, the PHRRs of samples PPAF3 and PPAF4 were, respectively, 240 and 310 kW/m^2 less than that of pure PP, corresponding to drops of 38 and 50%, respectively, compared with pure PP. The total heat releases (THRs) of samples PPAF3 and PPAF4 were 27 and 24 MJ/m^2, respectively, which were much smaller than that of pure PP, whose THR value was 46 MJ/m^2. It was indicated that the presence of AF effectively improved the fire performance of the PP composite; this was attributed to the increasing char layers formed by AFs, which could delay the spread

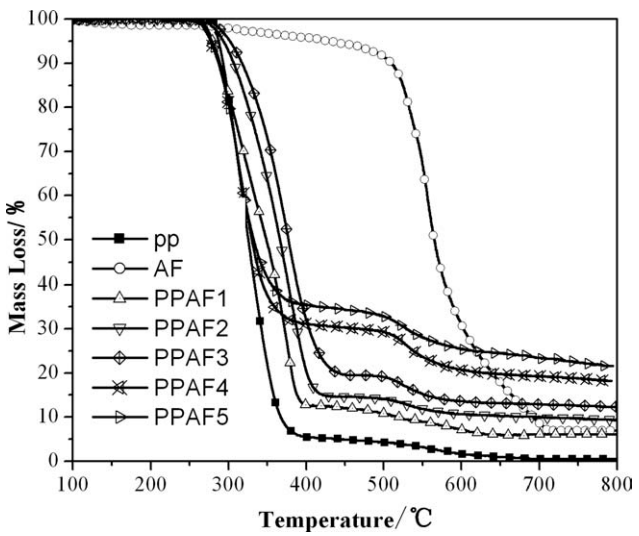

Figure 11 TGA curves of the pure PP and AF and PP/AF composites.

TABLE IV
Key Data of the Pure PP and AF and PP/AF Composites Obtained from the TGA Curves

Sample	Degradation temperature (°C)	Char residue at 700°C (%)
PP	271.3–400.4	0
AF	503.2–707.6	6.5
PPAF1	260.3–397.8 467.9–624.2	6.1
PPAF2	265.6–424.9 492.4–605.3	10.1
PPAF3	273.9–446.4 497.6–610.6	12.9
PPAF4	255.1–395.2 495.0–648.7	19.6
PPAF5	257.7–397.8 476.2–645.6	23.5

TABLE V
Comparison of the Flammability Properties among the Pure PP and PP/AF Composites

Sample name	LOI	UL-94	Dripping
PP	18.0	No rating	Yes
PPAF1	18.2	No rating	No
PPAF2	18.3	No rating	No
PPAF3	18.3	No rating	No
PPAF4	18.4	No rating	No
PPAF5	18.4	No rating	No

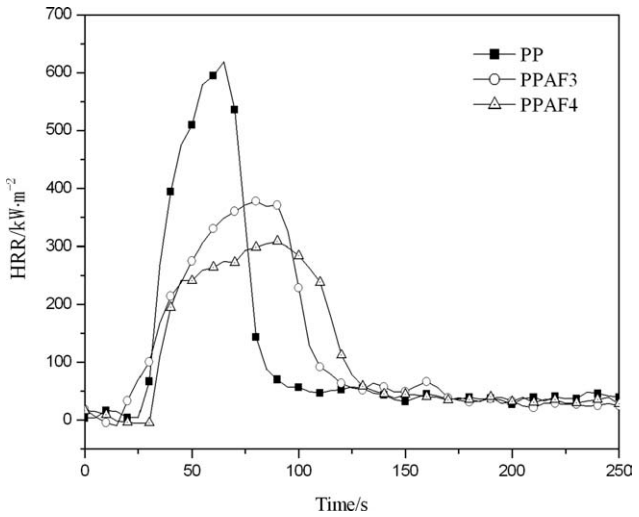

Figure 12 HRR curves of the pure PP, PPAF3, and PPAF4.

and exchange of heat flux and, hence, hindered the combustion rate.

CONCLUSIONS

The mechanical properties, including the tensile strength and izod notched impact strength, of the PP/AF composites were considerably enhanced by the introduction of AFs with an appropriate loading of 20 wt %. The presence of fibers improved the crystalline degree and speed by acting as heterogeneous nucleation sites and led to smaller and more integrated spherulites arrayed densely. Besides, AFs had positive effects on improving the thermal stability and flame retardancy of the PP/AF composites, especially on melt-dripping resistance and decreasing HRR and THR.

References

1. Zhang, S.; Horrocks, A. R. Prog Polym Sci 2003, 28, 1517.
2. Chen, X. S.; Yu, Z. Z.; Liu, W.; Zhang, S. Polym Degrad Stab 2009, 94, 1520.
3. Maity, J.; Jacob, C.; Das, C. K.; Alam, S.; Singh, R. P. Compos A 2008, 39, 825.
4. Zhang, S.; Horrocks, A. R.; Hull, R.; Kandola, B. K. Polym Degrad Stab 2006, 91, 719.
5. Zhang, S.; Hull, T. R.; Horrocks, A. R. Polym Degrad Stab 2007, 92, 727.
6. Kitagawa, K.; Hayasaki, S.; Ozaki, Y. Vib Spectrosc 1997, 15, 43.
7. Alonso, M. V.; Auad, M. L.; Nutt, S. Compos A 2006, 37, 1952.
8. Kukureka, S. N.; Hooke, C. J.; Rao, M.; Liao, P.; Chen, Y. K. Tribology Int 1999, 32, 107.
9. Abdulkadir, G.; Ahmet, O.; Emin, O. Mater Des 2006, 27, 316.
10. Chocronbenloulo, L. S.; Rodriguez, J.; Martinez, M. A.; Sanchezgalvez, V. Int J Impact Eng 1996, 19, 135.
11. Walker, L.; Hu, X. Z. Scr Mater 1999, 41, 575.
12. Lee, N. J.; Jang, J. Compos A 1999, 30, 815.
13. Thomason, J. L.; Vlug, M. A.; Schipper, G.; Krikort, H. G. L. T. Compos A 1996, 27, 1075.
14. Thomason, J. L. Compos A 2002, 33, 1641.
15. Mäder, E.; Moos, E.; Karger-Kocsis, J. Compos A 2001, 32, 631.
16. Arroyo, M.; Lopez-Manchado, M. A.; Avalos, F. Polymer 1997, 38, 5587.
17. Avalos, F.; Lopez-Manchado, M. A.; Arroyo, M. Polymer 1998, 39, 6173.
18. Pompe, G.; Mäder, E. Compos Sci Technol 2000, 60, 2159.
19. Zhuang, R. C.; Burghardt, T.; Mäder, E. Compos Sci Technol 2010, 70, 1523.
20. Thomason, J. L.; Schoolenberg, G. E. Composites 1994, 25, 197.
21. Cabral-Fonseca, S.; Paiva, M. C.; Nunes, J. P.; Bernardo, C. A. Polym Test 2003, 22, 907.
22. Vallittu, P. K.; Lassila, V. P.; Lappalainen, R. J Prosthet Dent 1994, 71, 607.
23. Thomason, J. L.; Vlug, M. A. Compos A 1996, 27, 417.
24. Thomason, J. L.; Groenewoud, W. M. Compos A 1996, 27, 555.
25. Stipho, H. D. J Prosthet Dent 1998, 80, 546.
26. Ladizesky, N. H.; Cheng, Y. Y.; Chow, T. W.; Ward, I. M. Dent Mater 1993, 9, 128.
27. Dyer, S. R.; Lassila, L. V. J.; Jokinen, M.; Vallittu, P. K. Dent Mater 2004, 20, 947.
28. Vallittu, P. K. J. Oral Rehabil 1995, 22, 257.
29. Arroyo, M.; Zitzumbo, R.; Avalos, F. Polymer 2000, 41, 6351.
30. Pompe, G.; Mader, E. Compos Sci Technol 2000, 60, 2159.
31. Thomason, J. L.; Rooyen, A. A. J Mater Sci 1992, 27, 889.
32. Wang, C.; Liu, C. R. Polymer 1999, 40, 289.
33. Cui, X. Y.; Zhou, X. D.; Dai, G. Plast Sci Technol 2000, 3, 14.
34. Lusziger, A.; Marrzinaky, C. N.; Mueller, R. R.; Wagner, H. D. Polym Mater Sci Eng 1997, 76, 170.
35. Nuriel, H.; Kozlovich, N.; Feldman, Y.; Marom, G. Compos A 2000, 31, 69.
36. Saikrasuna, S.; Amornsakchaia, T.; Sirisinhaa, C.; Meesirib, W.; Limcharoena, B. S. Polymer 1999, 40, 6437.
37. Larin, B.; Avila-Orta, A. C.; Somani, H. R.; Hsiao, S. B.; Marom, G. Polymer 2008, 49, 295.
38. Amornsakchaia, T.; Sinpatanapana, B.; Limcharoena, B. S. Polymer 1999, 40, 2993.
39. Zhang, Z. S.; Tao, Y. J.; Yang, Z. G.; Mai, K. C. Eur Polym J 2008, 44, 1955.
40. Zheng, Y. Y.; Wang, C. Y.; Fu, M. L. Polym Mater Sci Eng 2006, 22, 126.
41. Chattopadhyay, S. K.; Khandal, R. K.; Uppaluri, R.; Ghoshal, A. K. J Appl Polym Sci 2009, 113, 3750.
42. Aykol, M.; Isitman, A. N.; Firlar, E.; Kaynak, C. Polym Compos 2008, 29, 644.
43. Vuillequez, A.; Lebrun, M.; Ion, R. M.; Youssef, B. Macromol Symp 2010, 290, 146.
44. Wang, S. W.; Yang, W.; Xu, Y. J.; Xie, B. H.; Yang, M. B.; Peng, X. F. Polym Test 2008, 27, 638.
45. Zhao, S. C.; Cai, Z.; Xin, Z. Polymer 2008, 49, 2745.
46. Zheng, Y. Y.; Wang, C. Y.; Fu, M. L. J Aeron Mater 2006, 26, 51.
47. Liao, K. T.; Lu, Z. J.; Zheng, X. P. Polym Mater Sci Eng 1995, 11, 75.
48. Cui, X. Y.; Zhou, X. D.; Gance, I. D. Polym Mater Sci Eng 2002, 18, 138.